

Dynamic Models Including Uncertainty

AFOSR FINAL TECHNICAL REPORT FA9550-08-1-0147

For the period: February 1, 2008–November 30, 2008
submitted to

Air Force Office of Scientific Research
Attn: Dr. F. Fahroo and Dr. W. McEneaney, Dynamics and Control
Phone (703) 696-7796 Fax (703) 696-8450
875 N. Randolph St, Suite 325, Room 4111
Arlington, VA 22203-1768

January 22, 2009

PI:

Dr. H.T. Banks
North Carolina State University
Center for Research in Scientific Computation
Box 8212
Raleigh, NC 27695-8212
htbanks@ncsu.edu

20090319164

REPORT DOCUMENTATION PAGE

The public reporting burden for this collection of information is estimated to average 1 hour per response, including the time for reviewing instructions, searching existing data sources, gathering and maintaining the data needed, and completing and reviewing the collection of information. Send comments regarding this burden estimate or any other aspect of this collection of information, including suggestions for reducing the burden, to the Department of Defense, Executive Service Directorate (0704-0188). Respondents should be aware that notwithstanding any other provision of law, no person shall be subject to any penalty for failing to comply with a collection of information if it does not display a currently valid OMB control number.

PLEASE DO NOT RETURN YOUR FORM TO THE ABOVE ORGANIZATION.

1. REPORT DATE (DD-MM-YYYY) 31-01-2009	2. REPORT TYPE Final Technical	3. DATES COVERED (From - To) 01-02-2008 to 30-11-2008		
4. TITLE AND SUBTITLE Grant Title: DYNAMIC MODELS INCLUDING UNCERTAINTY		5a. CONTRACT NUMBER		
		5b. GRANT NUMBER FA9550-08-1-0147		
		5c. PROGRAM ELEMENT NUMBER		
6. AUTHOR(S) H. T. Banks		5d. PROJECT NUMBER		
		5e. TASK NUMBER		
		5f. WORK UNIT NUMBER		
7. PERFORMING ORGANIZATION NAME(S) AND ADDRESS(ES) North Carolina State University Center for Research in Scientific Computation Box 8212 Raleigh, NC 27695-8212		8. PERFORMING ORGANIZATION REPORT NUMBER		
9. SPONSORING/MONITORING AGENCY NAME(S) AND ADDRESS(ES) Air Force Office of Scientific Research <i>/NL</i> 875 North Randolph Street Suite 325, Rm 3112 Arlington, VA 22203 <i>Dr Wm McNeaney</i>		10. SPONSOR/MONITOR'S ACRONYM(S) AFOSR		
		11. SPONSOR/MONITOR'S REPORT NUMBER(S)		
12. DISTRIBUTION/AVAILABILITY STATEMENT <i>U</i> <i>Distribution A</i>				
13. SUPPLEMENTARY NOTES				
14. ABSTRACT In this 10 month funded effort, we report progress on the development of methods in a number of specific areas: stochastic and deterministic models for complex networks and development of inverse problem methodologies (generalized sensitivity functions). These efforts are part of our continuing fundamental research program in a modeling, estimation and control methodology(theoretical, statistical and computational) for systems in the presence of major model and observation uncertainties.				
15. SUBJECT TERMS stochastic and deterministic models for complex networks; inverse problem methodologies; generalized sensitivity functions				
16. SECURITY CLASSIFICATION OF: a. REPORT U b. ABSTRACT U c. THIS PAGE U		17. LIMITATION OF ABSTRACT UU	18. NUMBER OF PAGES 27	19a. NAME OF RESPONSIBLE PERSON H. T. Banks
				19b. TELEPHONE NUMBER (Include area code) 919-515-3968

ABSTRACT

In this 10 month funded effort, we report progress on the development of methods in a number of specific areas: stochastic and deterministic models for complex networks and development of inverse problem methodologies (generalized sensitivity functions). These efforts are part of our continuing fundamental research program in a modeling, estimation and control methodology (theoretical, statistical and computational) for systems in the presence of major model and observation uncertainties.

1 Brief Overview Summary

Motivated by examples in viscoelasticity and biomedicine such as in [P5,P6,P7], we consider in [P2] the problem of estimating a modeling parameter θ using a least squares criterion $J_d(y, \theta) = \sum_{i=1}^n (y(t_i) - f(t_i, \theta))^2$. We take an *optimal design* perspective in [P2]. Our general premise (illustrated via examples in [P2]) is that in any data collected, the information content with respect to estimating θ may vary considerably from one time measurement to another, and in this regard some measurements may be much more informative than others. We propose mathematical tools which can be used to collect data in an *almost optimal* way, by specifying the duration and distribution of time sampling in the measurements to be taken, consequently improving the accuracy (i.e., reduce the uncertainty in estimates) of the parameters to be estimated.

We recall the concepts of *traditional* and *generalized sensitivity functions* and use these to develop a strategy to determine the “optimal” duration time T for an experiment; this is based on the time evolution of the sensitivity functions and of the condition number of the Fisher information matrix. We illustrate the role of the sensitivity functions as tools in optimal design of experiments, in particular in finding “best” sampling distributions. We also present a new optimal design criterion which is based on the idea of finding the time distribution which gives the best discrete approximation for the integral version of the Fisher information matrix. Numerical examples are presented throughout [P2] to motivate and illustrate the ideas. Theoretical foundations are presented in an appendix of [P2].

Alternative but related methods for optimal design of experiments are presented and explored in [P4].

Stochastic differential equation (SDE) models offer one formulation for introducing uncertainty in human interactions in a dynamic social network model based on static and/or deterministic ordinary differential equation (ODE) models. A coupled SDE system for agent characteristics and connectivities was developed and investigated in [7]. This SDE model (which tacitly assumed instantaneous influence between agents with connectivity) may be improved by including delays in an SDE model or in an equivalent Fokker-Planck (FP) model if such exists. The coupled model of [7] involved discontinuities and did not yield a

Markov diffusion process (for which an equivalent Fokker-Planck formulation is possible). In this effort we formulate a new smooth vector SDE system and demonstrate that it generates a Markov diffusion process and provides computational results equivalent to those of the earlier model of [7]. The new model is compared to the earlier model via simulations. We derive an equivalent Fokker-Planck formulation to this new SDE system. Numerical methods to implement the FP model are being formulated and tested. Versions of these equivalent models will be modified first to include deterministic delays and then delays with some stochasticity/uncertainty.

1.1 Publications supported in part under this grant

- [P1] H. T. Banks and M. Pedersen, Well-posedness of inverse problems for systems with time dependent parameters, CRSC-TR08-10, August, 2008; *Arabian Journal of Science and Engineering: Mathematics*, to appear.
- [P2] H.T. Banks, Sava Dedić, Stacey L. Ernstberger and Franz Kappel, A new approach to optimal design problems, CRSC-TR08-12, September, 2008; *Inverse Problems*, submitted.
- [P3] H.T. Banks, J.E. Banks and S. L. Joyner, Estimation in time-delay modeling of insecticide-induced mortality, CRSC-TR08-15, October, 2008; *J. Inverse and Ill-posed Problems*, submitted.
- [P4] H.T. Banks, J.L. Davis, S.L. Ernstberger, S. Hu, E. Artimovich, and A.K. Dhar, Experimental design and estimation of growth rate distributions in size-structured shrimp populations, CRSC-TR08-20, November, 2008; *Inverse Problems*, submitted.
- [P5] H.T. Banks and J.R. Samuels, Jr., Detection of cardiac occlusions using viscoelastic wave propagation, CRSC-TR08-23, December, 2008; *Advances in Applied Mathematics and Mechanics*, submitted.
- [P6] D. Valdez-Jasso, H.T. Banks, M.A. Haider, D. Bia, Y. Zocalo, R.L. Armentano, and M.S. Olufsen, Viscoelastic models for passive arterial wall dynamics, CRSC-TR08-24, December, 2008; *Advances in Applied Mathematics and Mechanics*, submitted.
- [P7] H.T. Banks, Kathleen Holm, Nathan C. Wanner, Ariel Cintrón-Arias, Grace M. Kepler and Jeffrey D. Wetherington, A mathematical model for the first-pass dynamics of antibiotics acting on the cardiovascular system, CRSC-TR08-25, December, 2008; *Mathematical and Computer Modeling*, submitted.
- [P8] H. T. Banks, K. L. Rehm and Karyn Sutton, Dynamic social network models with stochasticity and delays, in preparation.

2 Personnel Supported (at least in part with this grant)

- H.T. Banks, Prof., North Carolina State University
- G. M. Kepler, Res. Assoc., North Carolina State University
- S. Dedić, Post doc, North Carolina State University

- S. Hu, Post doc, North Carolina State University
- K. Sutton, Post doc, North Carolina State University,
- S. Joyner, Graduate Student at North Carolina State University
- J. Samuels, Graduate Student at North Carolina State University

3 Relevance of Research to DOD/AF Missions

The development of general classes of nonlinear complex nodal network models with inherent uncertainties is directly relevant to several recently announced “Discovery Challenge Thrusts” in AFOSR-BAA-2007-08. In particular, our efforts will address basic research issues that will be related to the programs announced on “Robust Decision Making” and “Complex Networked Systems” which are concerned with operational environments where “unexpected events, attacks on and degradations of the network centric system and sudden changes in goals and objectives” must be accommodated. The need for new modeling paradigms which include robustness in estimation and control in models with uncertainty is well recognized.

We expect the developed methodologies to be of direct interest to scientists and engineers in the Information Directorate at AFRL, Rome, NY, in their ongoing efforts on information nodal network systems, security and information warfare.

4 Detailed Research Summaries

4.1 Generalized Sensitivity and Optimal Design

We consider first a parameter estimation problem for the general nonlinear dynamical system

$$\begin{aligned}\dot{x}(t) &= g(t, x(t), \theta) \\ x(t_0) &= x_0,\end{aligned}\tag{4.1}$$

with discrete time observations

$$y_j = f(t_j, \theta) + \epsilon_j = Cx(t_j, \theta) + \epsilon_j, \quad j = 1, \dots, n\tag{4.2}$$

where $x, g \in \mathbb{R}^N$, $f, \epsilon_j \in \mathbb{R}^M$ and $\theta \in \mathbb{R}^p$. The matrix C is an $M \times N$ matrix which gives the observation data in terms of the components of the state variable x .

Generalized sensitivity functions (GSFs) were introduced recently by Thomaseseth and Cobelli [26] as a new tool in identification studies to analyze the distribution of the information content (with respect to the model parameters) of the output variables of a system for a

given set of observations. More precisely, the generalized sensitivity functions describe the sensitivity of the *parameter estimates* obtained from an inverse problem with respect to the *data measurements* used in the inverse problem.

For a scalar observation model with discrete time measurements (i.e., when $M = 1$ and C is a $1 \times N$ array in (4.2)), the generalized sensitivity functions (GSFs) are defined as

$$\mathbf{gs}(t_l) = \sum_{i=1}^l \frac{1}{\sigma^2(t_i)} [F^{-1} \times \nabla_\theta f(t_i, \theta_0)] \bullet \nabla_\theta f(t_i, \theta_0), \quad (4.3)$$

where $\{t_l\}$, $l = 1, \dots, n$, is the time distribution where the measurements are taken,

$$F = \sum_{j=1}^n \frac{1}{\sigma^2(t_j)} \nabla_\theta f(t_j, \theta_0) \nabla_\theta f(t_j, \theta_0)^T \quad (4.4)$$

is the corresponding Fisher information matrix, and θ_0 is the usual “true” parameter value tacitly assumed to exist in standard statistical theories. The symbol “ \bullet ” represents element-by-element vector multiplication. For the motivation and details which led to the definition above, the reader should consult [26] and [11]. The Fisher information matrix measures the information content of the data corresponding to the model parameters. In (4.3) we see that this information is transferred to the GSFs, making them appropriate tools to indicate the relevance of the measurements to the estimates obtained in parameter estimation problems.

We note that the generalized sensitivity functions (4.3) are vector-valued functions having the same dimension as the parameter θ being estimated. The k -th component of the vector function \mathbf{gs} represents the generalized sensitivity function with respect to θ_k . The GSFs are defined only at the discrete time points $\{t_j, j = 1, \dots, n\}$ and they are cumulative functions, at each time point t_l taking into account only the contributions to estimates of the measurements up to t_l , thus indicating the influence of measurements up to that time on the parameter estimates obtained.

From (4.3) it is readily observed that all the components of \mathbf{gs} are one at the end of the total time interval, i.e., $\mathbf{gs}(t_M) = \mathbf{1}$. If one defines $\mathbf{gs}(t) = \mathbf{0}$ for $t < t_1$ (\mathbf{gs} is zero when no measurement is collected), then each component of \mathbf{gs} varies from 0 to 1 during the experiment. As developed in [26], the time subinterval during which this transition has the *sharpest increase* corresponds to measurements which provide the most information on possible variations in the corresponding estimated model parameters. The amount of information with respect to a parameter θ_k is directly related to the rate of change of the corresponding GSF; thus sharp increases in \mathbf{gs}_k indicate a high rate in additional information about θ_k being provided by the new measurements in that time period.

For finite dimensional systems ($N < \infty$) with a finite number ($p < \infty$) of parameters, the numerical implementation of the generalized sensitivity functions (4.3) is straightforward, since the gradient of f with respect to θ (or x_0) is simply the Jacobian of x with respect to θ (or x_0) multiplied by C . These Jacobian matrices can be obtained by numerically solving sensitivity ODE systems coupled with the system (4.1).

We have effectively used GSFs in several problems [10, 4] with finite dimensional parameters in ordinary differential equation systems. The primary contribution of generalized sensitivity functions is that they can indicate regions of high information content where, if additional data points are taken, one can generally improve the existing parameter estimates. This has rather obvious applications to experimental design. Moreover, by visually investigating the dynamics of GSF curves, one can potentially identify subsets of parameters which are highly correlated. While there are still some heuristics underlying the development of GSFs (the presentation in the appendices of [5, 11] offers the most rigorous presentation to date), it is clear that some version of the GSF theory should become a valuable tool for scientific and engineering investigators needing to estimate parameters in dynamical systems. Although the GSF theory provides useful information in parameter estimation, the most insight can be gained when the GSFs are used in conjunction with traditional sensitivity functions.

In order to illustrate our ideas, we changed the traditional order of the steps, and we assume that we need to estimate the parameter θ from a set of observations of the output variable $y = Cx$ which are not known *a priori*. Indeed, let us assume that the only things we know for the moment are the physical problem and the mathematical model (4.1)–(4.2) used to model it, but we have the freedom to instruct the experimentalists as to the number of observations to take, and more importantly at what times to take them. We also assume that the underlying model (4.1)–(4.2) is a good representation of the physical problem (i.e., there is agreement between the observed data and the corresponding values generated by (4.1)–(4.2) with an appropriate choice of θ), and that we have a criterion to ascertain the quality of the estimates obtained (for instance, the standard errors). Given these assumptions, it makes sense, once we have a mathematical model and an algorithm to perform the inversion (least squares for example), to look for a strategy for collecting experimental data in the best possible way. We want to take maximum advantage of the mathematical structure of the model in order to indicate the optimal number of observations to take, as well as their optimal temporal distribution, thus obtaining better accuracy for the estimates.

Some of the most important questions in parameter estimation problems when considering the dynamical system (4.1)–(4.2) are:

1. How do we choose the duration T of the experiment, or the interval $[0, T]$ from where to sample data, in order to obtain the best estimates for θ ?
2. Once the duration T is established, what is the optimal sampling distribution of an *a priori given* number of measurements in the interval $[0, T]$, in order to obtain the most accurate estimates?

The first question hints to the minimum time interval which contains most of the relevant information with respect to the estimation of θ . The second question constitutes the main topic of the optimal experimental design literature, and the traditional way to answer it is to find time distributions which optimize some specific “design” functions. In general, an optimal design minimizes or maximizes a given function of the Fisher information matrix.

However, this matrix depends on the true parameter θ_0 , which in practice is unknown. In order to overcome this difficulty one usually substitutes an initial guess θ^* for θ_0 . The resulting designs are called locally optimal designs. Of the numerous design strategies found in the literature (for example, see [12, 17, 18, 24]) we briefly enumerate here the most popular, which are:

- a) the *D-optimal design*, which arguably maximizes the determinant $\det F(\theta^*)$ of the Fisher information matrix. It is largely accepted in the literature because of its appealing geometrical interpretation: the asymptotic confidence regions for the maximum likelihood estimate of θ are ellipsoids. One can show that an optimal design with respect to this criterion yields approximately a minimal value for the volume of the tolerance ellipsoid of the estimates;
- b) the *c-optimal design*, which minimizes the variance of a linear combination $g(\theta) = c^\top \theta$ of the parameters to be estimated. Up to a multiplicative constant, the asymptotic covariance of the maximum likelihood of g is given by $c^\top F^{-1}(\theta^*)c$, and an optimal design with respect to this criterion minimizes this variance. In the particular case when c is the i -th unit vector, i.e., $c = e_i$, the *c*-optimal design minimizes the variance of the least squares estimate for the i -th parameter θ_i ;
- c) the *E-optimal design*, which maximizes the smallest eigenvalue $\lambda_{\min}(F(\theta^*))$ of the Fisher information matrix. This is equivalent to minimizing the maximum eigenvalue $\lambda_{\max}(F^{-1}(\theta^*))$ of the inverse F^{-1} (the covariance matrix), or to minimizing the worst variance among all estimates $c^\top \hat{\theta}$ for the linear combinations $c^\top \theta$ with a given norm $c^\top c = 1$. Geometrically, the *E*-optimal design minimizes the maximum diameter of the asymptotic confidence ellipsoids for θ .

The practical importance of the issues addressed by the previous two questions is obvious for those experiments where the cost of measurements (invasive procedures, expensive technology, necessity of highly qualified personnel, etc.) is high and where one wants to avoid running the experiments longer than necessary. These questions suggest that we investigate the temporal distribution of the information content with respect to parameters we want to estimate, the sensitivity of the model output and of the parameter estimates with respect to model parameters, and lead us to introduce mathematical tools which to describe them.

Our strategy in answering the previous questions is to assume that we have continuous time measurements in $[0, T]$ and develop tools to quantify the information content with respect to θ (imbedded in η) throughout the interval $[0, T]$. In order to carry this out, we reformulate the estimation problem by using an integral form of the least squares, integral optimality conditions, and integral version of the Fisher information matrix (its integral form on the interval $[0, T]$). First we show that the *traditional and generalized sensitivity functions* (GSF) can indicate regions of high information content, where if additional data points are sampled, the corresponding parameter estimates are improved (as we have noted GSF were introduced first, to our knowledge, by Thomaseth and Cobelli, see [4, 11, 26]). Therefore we advocate their utilization as new tools in experimental design. In [5] we propose a new

optimal design strategy which is based on the idea of finding a discrete sampling distribution on $[0, T]$, which best approximates the integral version of the Fisher information matrix with a discretized version. To carry this out, we formulate in [5] a new continuous GSF based on probability distributions representing the sampling which can then be optimized over the metric space of probability measures formulated with the Prohorov metric [2, 23].

4.2 Nodal Networks with Uncertainty

Networks with uncertainty are ubiquitous in science and engineering, but especially in complex nonlinear systems of interest to DOD. In particular, nodal networks with uncertainty are fundamental to the understanding of problems involving *dynamic resource management and allocation*. Examples range from service scheduling and material supply chains to production systems and modern high speed communication networks where information is routed between nodes in a distributed information system with a global grid.

Social network structures can be represented by graphs in which individuals, or agents, are represented by vertices and the connections between agents are represented by edges. Agents are defined by measurable *characteristics*, and the connections between agents can be defined as either unidirectional, thus creating a directed graph, or bidirectional, thus creating an undirected graph. In social network graphs, the relationship between two agents, or a pairwise relationship, is considered to be the most basic structure used in constructing the graph. More complicated social models, even triads including three agents, are created from using multiple pairwise relationships. Research on social networks may be applied to many areas, including social group structure, information sharing, and disease outbreak.

Interactions between agents often have uncertain and unpredictable results, and many static and deterministic social network models fail to consider variability and delay. Complex nonlinear systems are more suited for modeling the uncertainty found in human interactions. A dynamic social network model that includes delay and accounts for variability could allow governmental organizations to predict the propagation of information through a terrorist network [2], allow local officials to examine how a communicable disease would spread through their community [20], or enable corporations to simulate scenarios in which their supply chain operates under strained conditions or with perturbations [10].

One area of current research in social networks is dynamics of connections and agents over a time. The model first proposed by [7] utilizes a coupled system of stochastic differential equations (SDE's). Agents are defined by quantitatively described characteristics and the strength of the pairwise relationship, or *degree of connectivity*, joining two agents is determined by these characteristics. It is assumed that agents participate in *homophilic* relationships and that two agents are more likely to have a positive degree of connectivity if their characteristics are similar. The proposed model accounts for changes in agents and relationships through both observable interactions and unobservable events represented as noise.

Another factor in social network dynamics that can be considered is delay. The effect one agent has on another often is not instantaneous; like diseases in a body, new ideas and

opinions are subject to a propagation time in an agent's mind before the agent accepts or rejects the new concept. An agent does not pass on ideas, objects, and diseases immediately after they have come in contact with or possession of them. Consider a conversation between two people of differing religious views. It is unlikely that one will immediately convert to the other's faith; however, after repeated contact and reflection by each individual, the two may become more understanding of each others' religions. Adding constant and stochastic delays to the proposed model will result in a more realistic simulation of agent interactions and internal changes in the agents.

The proposed model is built from the model created by [7]. The model is used with the assumption that time, degrees of connectivity, and agent characteristics are continuous. The coupled SDE model proposed in [7] was revisited and used to reproduce previous results. The SDE's were then changed so that the coefficients used in the model are smooth, allowing the model to satisfy the conditions of a diffusion process, and the results of the model with smooth coefficients are compared to the results of the original model to verify that the change in coefficients does not affect the visible behavior of the model. These equations are then converted to an equivalent Fokker-Planck (FP) model. Numerical implementation of the FP model as an alternative modeling and numerical approach, with attention to ability to add delays to the system, is under investigation.

4.2.1 Basic Stochastic Differential Equation Model

Denote the vector of characteristics of agent i , $i \in \mathcal{N} = 1, \dots, N$ at time t by $\mathbf{C}_i(t) \in K \subset \mathbb{R}^m$, where K is a compact constraint set for the values of characteristics and m is the number of characteristics. Refer to the degree of connectivity between agent i and agent i' at time t by $e(i, i', t) \in \mathbb{R}$ such that an agent's connectivity to itself $e(i, i, t) = 0 \forall i, t$ and an edge between i and i' exists if and only if $e(i, i', t) > 0$. The strength of the link between agent i and agent i' is not bidirectional, so it is possible that $e(i, i', t) \neq e(i', i, t)$. Define $A_i(t) = \{i' \in \mathcal{N} : e(i, i', t) > 0\}$ to be the set of all agents to which agent i is linked at time t , and let $|A_i(t)|$ be the number of elements in $A_i(t)$.

The system of coupled stochastic differential equations as defined by [7] used as the starting point in this model are

$$d\mathbf{C}_i(t) = \frac{\beta_i}{|A_i(t)|} \sum_{i' \in A_i(t)} [\mathbf{C}_{i'}(t) - \mathbf{C}_i(t)] dt + \sigma d\mathbf{W}_i^C(t) \quad (4.5)$$

$$de(i, i', t) = f(\|\mathbf{C}_i - \mathbf{C}_{i'}\|^2) dt + \gamma d\mathbf{W}_{i,i'}^e(t). \quad (4.6)$$

In (4.5), the constant β_i is an agent-specific value that represents the desire of agent i to be more like agents to which it is linked and $\sigma \mathbf{W}_i^C(\cdot)$ is a Wiener process with variance σ^2 . In (4.6), $f(\xi) = 2e^{-b\xi} - 1$ where the constant $b > 0$ controls the rate at which edges are formed and $\|\cdot\|^2$ denotes the square of the vector norm in \mathbb{R}^m , and $\gamma d\mathbf{W}_{i,i'}^e(\cdot)$ is a Wiener process with variance γ^2 .

4.2.2 Stochastic Differential Equation with Smooth Coefficients

The model described by (4.5) does not fit the definition of a usual diffusion process because the values of $|A_i(t)|$ change discontinuously. An alternative model is proposed in [7]:

$$d\mathbf{C}_i(t) = \frac{\beta_i}{\sum_{i' \neq i} e(i, i', t)} \sum_{i' \neq i} e(i, i', t) [\mathbf{C}_{i'}(t) - \mathbf{C}_i(t)] dt + \sigma d\mathbf{W}_i^C(t) \quad (4.7)$$

The sum $\sum_{i' \neq i} e(i, i', t)$ is defined for all sums of all possible values of $e(i, i', t)$ and thus is continuous. While it has smooth coefficients, this model fails to follow the assumption of homophily and enables agents who have a non-positive connectivity to a particular agent to influence the characteristics of that particular agent. This in turn causes the degrees of connectivity $e(i, i', t(n)) \rightarrow \infty$ as $n \rightarrow \infty$, resulting in single cluster scenarios for any value of b in the deterministic case, as illustrated by Figure 1.

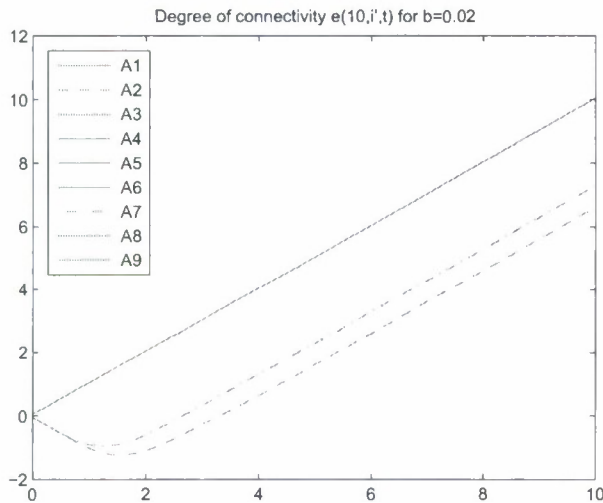


Figure 1: Degree of connectivity $e(10, i', t)$, $i' \neq 10$ of agent 10 with other agents for $b = 0.02$ using smooth model proposed in [7].

Consider the agents $i', i' \neq 2, 7$ and agent 2 in the case study used in [7] in which $\mathbf{C}_{i'}(0) = (10, 10)$ and $\mathbf{C}_2(0) = (-10, -10)$. Assume that these agents' characteristics remain the same for several time steps in the simulation while the degrees of connectivity $e(i', 2, t)$ and $e(2, i', t)$ become negative numbers so that $e(2, i', t_n) = -1.5$ at some time t_n . Ignoring agent 7, (4.7) would reduce in the deterministic case to

$$\begin{aligned}
d\mathbf{C}_2(t_n) &= \frac{\beta}{\sum_{i' \neq 2} e(2, i', t_n)} \sum_{i' \neq 2} e(2, i', t_n) [\mathbf{C}_{i'}(t_n) - \mathbf{C}_2(t_n)] dt \\
&\quad + \sigma d\mathbf{W}_i^C(t_n) \\
d\mathbf{C}_2(t_n) &= \frac{1}{-12} \sum_{i' \neq 2} -1.5 \left[\begin{bmatrix} 10 \\ 10 \end{bmatrix} - \begin{bmatrix} -10 \\ -10 \end{bmatrix} \right] dt + 0 d\mathbf{W}_i^C(t_n) \\
d\mathbf{C}_2(t_n) &= \begin{bmatrix} 20 \\ 20 \end{bmatrix} dt
\end{aligned}$$

As noted before, agents to which agent 2 has a negative degree of connectivity should not alter the characteristic values of agent 2, but this rule is clearly violated by this proposed smooth model.

To avoid agents affecting each other at values of $e(i, i', t) \leq 0$, several augmentations to the sum $\sum_{i' \neq i} e(i, i', t)$ were considered. One proposed change that enabled the model to produce results similar to those produced by (4.5) was

$$d\mathbf{C}_i(t) = \frac{\beta_i}{\sum_{i' \in A_i(t)} e(i, i', t)} \sum_{\substack{i' \neq i \\ i' \in A_i(t)}} e(i, i', t) [\mathbf{C}_{i'}(t) - \mathbf{C}_i(t)] dt + \sigma d\mathbf{W}_i^C(t) \quad (4.8)$$

Like in (4.5), $A_i(t)$ is the set of agents $i' \neq i$ that have connectivity $e(i, i', t) > 0$. As the creation of $A_i(t)$ requires additional calculations and computer resources, this method is less efficient than the ideal method. Imposing the additional condition on the sum may also have unwanted effects when this equation is converted to a Fokker-Planck equation. The SDE system with smooth coefficients containing an equivalent method of expressing (4.8) is

$$d\mathbf{C}_i(t) = \frac{\beta_i}{\sum_{i' \neq i} \varphi} \sum_{i' \neq i} \varphi [\mathbf{C}_{i'}(t) - \mathbf{C}_i(t)] dt + \sigma d\mathbf{W}_i^C(t) \quad (4.9)$$

$$de(i, i', t) = f(\|\mathbf{C}_i - \mathbf{C}_{i'}\|^2) dt + \gamma d\mathbf{W}_{i,i'}^e(t). \quad (4.10)$$

In (4.8), $\varphi = \frac{1}{2}(e(i, i', t) + |e(i, i', t)|)$. As no agents i' are to affect agent i if $e(i, i', t) \leq 0$, it is assumed that $\frac{\beta_i}{\sum_{i' \neq i} \varphi} = 0$ if $\sum_{i' \neq i} \varphi = 0$. Thus this model will not fail if single-agent clusters arise during a simulation. This model maintains the requirement of *homophily* between agents and prevents agents with non-positive degrees of connectivity affecting other agents. When used to run simulations of the test cases first run with (4.5), results similar to those of the earlier model are produced.

4.2.3 Numerical Scheme for Stochastic Models

We continued to use the stochastic analogue of the classical fourth-order Runge-Kutta method to solve the system of differential equations as implemented by [7]. Approximating $d\mathbf{C}_i(t)$ remains nearly the same:

$$\mathbf{C}_i(t_n) = \mathbf{C}_i(t_{n-1}) + p_0 \mathbf{F}_0 h + p_1 \mathbf{F}_1 h + p_2 \mathbf{F}_2 h + p_3 \mathbf{F}_3 h + \sigma \Delta \mathbf{W}_{in}^C \quad (4.11)$$

where

$$\begin{aligned} \mathbf{F}_0 &= \mathbf{g}\left(t_{n-1}, \mathbf{C}_i(t_{n-1})\right) \\ \mathbf{C}_i^{(1)}(t_{n-1}) &= \mathbf{C}_i(t_{n-1}) + \frac{1}{2} \mathbf{F}_0 h + \frac{1}{2} \sigma \Delta \mathbf{W}_{in}^C \\ \mathbf{F}_1 &= \mathbf{g}\left(t_{n-1} + \frac{1}{2} h, \mathbf{C}_i^{(1)}(t_{n-1})\right) \\ \mathbf{C}_i^{(2)}(t_{n-1}) &= \mathbf{C}_i(t_{n-1}) + \frac{1}{2} \mathbf{F}_1 h + \frac{1}{2} \sigma \Delta \mathbf{W}_{in}^C \\ \mathbf{F}_2 &= \mathbf{g}\left(t_{n-1} + \frac{1}{2} h, \mathbf{C}_i^{(2)}(t_{n-1})\right) \\ \mathbf{C}_i^{(3)}(t_{n-1}) &= \mathbf{C}_i(t_{n-1}) + \mathbf{F}_2 h + \sigma \Delta \mathbf{W}_{in}^C \\ \mathbf{F}_3 &= \mathbf{g}\left(t_{n-1} + h, \mathbf{C}_i^{(3)}(t_{n-1})\right), \end{aligned}$$

$$p_0 = p_3 = \frac{1}{6} \text{ and } p_1 = p_2 = \frac{1}{3}.$$

The value of σ was added to the calculation of $\mathbf{C}_i^{(1)}(t_{n-1})$, $\mathbf{C}_i^{(2)}(t_{n-1})$, and $\mathbf{C}_i^{(3)}(t_{n-1})$ to scale the value of $\Delta \mathbf{W}_{in}^C$ so that it reflected the value of $\sigma \Delta \mathbf{W}_{in}^C$ used in (4.11). The definition of $\mathbf{g}(t, \mathbf{C}_i(t))$ is dependent upon the model. For approximation of the basic SDE, $\mathbf{g}(t, \mathbf{C}_i(t)) = \frac{\beta_i}{|A_i(t)|} \sum_{i' \in A_i(t)} [\mathbf{C}_{i'}(t) - \mathbf{C}_i(t)]$, and for the smooth coefficient SDE, $\mathbf{g}(t, \mathbf{C}_i(t)) = \frac{\beta_i}{\sum_{i' \neq i} \varphi} \sum_{i' \neq i} \varphi [\mathbf{C}_{i'}(t) - \mathbf{C}_i(t)]$.

Equation (4.6) may be solved using a simplified manner since its result is not dependent upon the value of the degree of connectivity $e(i, i', t)$. This can be expressed as

$$\begin{aligned} e(i, i', t_n) &= e(i, i', t_n) + p_0 f\left(\|\mathbf{C}_i(t_{n-1}) - \mathbf{C}_{i'}(t_{n-1})\|^2\right) h \\ &\quad + (p_1 + p_2) f\left(\|\mathbf{C}_i(t_{n-1}) + \frac{1}{2} h - \mathbf{C}_{i'}(t_{n-1}) + \frac{1}{2} h\|^2\right) h \\ &\quad + p_3 f\left(\|\mathbf{C}_i(t_n) - \mathbf{C}_{i'}(t_n)\|^2\right) h + \gamma \Delta \mathbf{W}_{in}^e. \end{aligned} \quad (4.12)$$

Here $\Delta \mathbf{W}_{in}^e = \mathbf{W}_{i,i'}^e(t_n) - \mathbf{W}_{i,i'}^e(t_{n-1})$ are standard Wiener increments with the distribution $N(0, h)$ where $h = \Delta t_n$. We assume that the value of $\mathbf{C}_i(t_n) + \frac{1}{2} h$ can be approximated linearly from $\mathbf{C}_i(t_{n-1})$ to $\mathbf{C}_i(t_n)$ when Δt_n is sufficiently small and therefore $\mathbf{C}_i(t_{n-1} + \frac{1}{2} h)$ may be approximated by $\frac{\mathbf{C}_i(t_{n-1}) + \mathbf{C}_i(t_n)}{2}$.

4.2.4 Numerical Simulations

We use the same case study concerning 10 agents as in [7] over a time interval of $t \in [0, 10]$. To avoid $\frac{\beta_i}{|A_i(0)|}$ being undefined, we calculate $e(i, i', 0) = f(\|\mathbf{C}_i(0) - \mathbf{C}_{i'}(0)\|^2)h$. This will cause all connectivities to start with a nonzero value that is also indicative of the sign of the degree of connectivity between two agents as determined by their characteristics.

4.2.5 Deterministic Case

The reproduction of the existing model performs similarly to that of the paper [7] in the deterministic case (when $\sigma = 0$ and $\theta = 0$). By properly implementing (4.6), the values of b that determined the number of clusters created after the same time as used in [7] were found to be different. One cluster formed when $b \in (0, 0.00155)$; two clusters formed when $b \in [0.00155, 0.01390)$; and three clusters formed when $b \in [0.01390, \infty)$. Two agents are members of different clusters if their connectivities $e(i, i', t) \leq 0$ and $e(i', i, t) \leq 0$. The clusters are identical to those described in [7]: the one cluster scenarios had a result of one cluster of all 10 agents; the two cluster scenarios had a result of one cluster of agents 2 and 7 and a second cluster of all other agents; and the three cluster scenario had a result of one cluster of only agent 2, one cluster of only agent 7, and one cluster of all other agents, and the degrees of connectivity between agents changed at a rate identical to the rates found in [7].

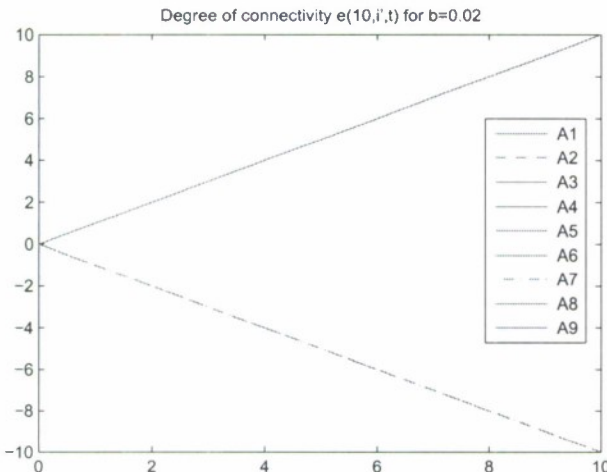


Figure 2: Degrees of connectivity $e(10, i', t)$, $i' \neq 10$ of agent 10 with other agents for $b = 0.02$ (three cluster scenario).

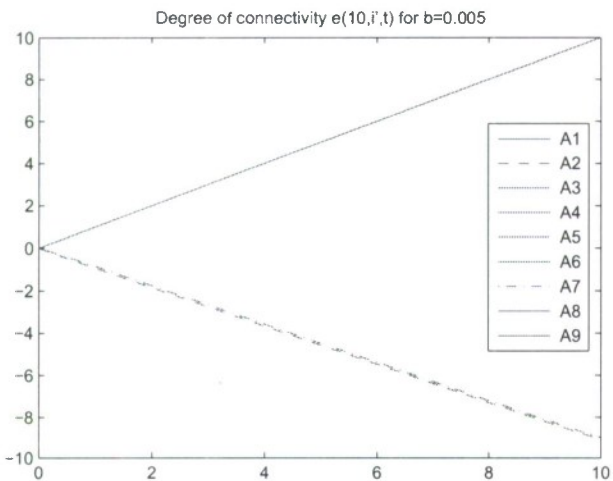


Figure 3: Degree of connectivity $e(10, i', t)$, $i' \neq 10$ of agent 10 with other agents for $b = 0.005$ (two cluster scenario).

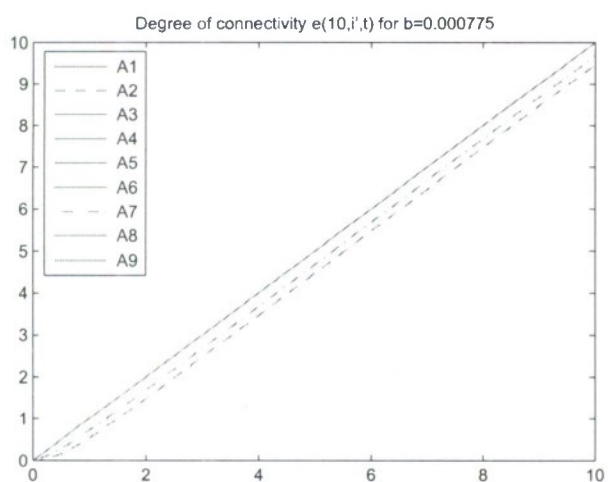


Figure 4: Degree of connectivity $e(10, i', t)$, $i' \neq 10$ of agent 10 with other agents for $b = 0.000775$ (one cluster scenario).

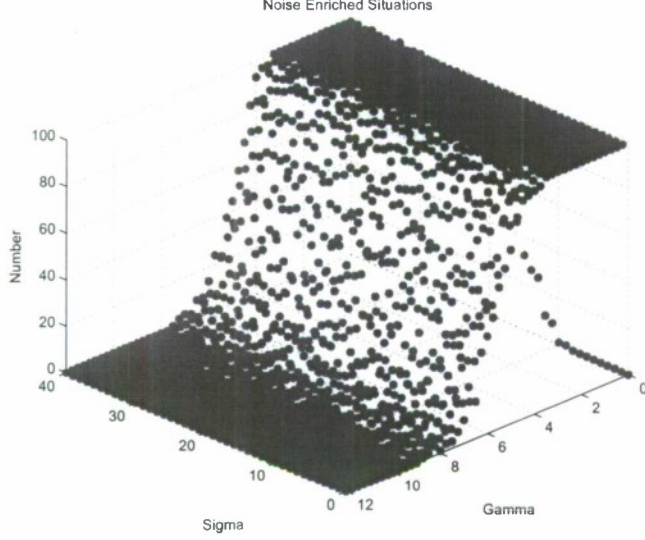


Figure 5: The (σ, γ) noise-enriched surface along $\sigma \in [0, 40]$, $\gamma \in [0, 12]$ plotted as a number out of 100 simulations.

4.2.6 Stochastic Case

Four regimes are defined in [7] into which the results of a simulated trial may be organized. These four regimes are labeled essentially deterministic, noise enriched, noise enlarged (with two- and three-cluster possibilities), and noise dominated.

To investigate the occurrence of the regimes defined in [7] using a constant b and variable σ and γ we ran simulations, with time step $h = \Delta t_n = 0.05$, for selected values of $\sigma \in [0, 40]$ and $\gamma \in [0, 12]$ with fixed $b = 0.000775$. We carried out 100 simulations for each pair (σ_k, γ_l) in a partition with values $\sigma_k = k = 0, 1, \dots, 40; \gamma_l = 0.25l, l = 0, 1, \dots, 48$. To further investigate the relationship between σ , δ , and the number of trials that produced essentially deterministic results, we also carried out 100 simulations for each pair (σ_k, γ_l) in a partition with values $\sigma_k = k = 0, 1, \dots, 40; \gamma_l = 0.0025l, l = 0, 1, \dots, 48$. The trends exhibited in [7] Figures 10 - 13 are also present in the charts produced by the proposed model albeit on a larger domain of σ and γ . Again, the surface of the noise-dominated regime is almost the complement of the surface of the noise-enriched regime with the exception of the occurrence of some essentially deterministic cases at low values of σ and γ . This indicates that it is highly unlikely that the inclusion of noise in the model will cause the simulation to reach a two- or three-clustered scenario if a b in the range of values that will produce a one-clustered scenario is selected.

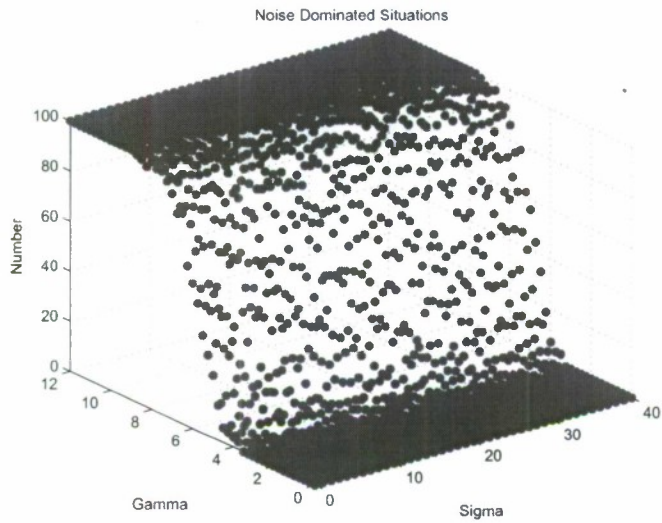


Figure 6: The (σ, γ) noise-dominated surface along $\sigma \in [0, 40]$, $\gamma \in [0, 12]$ plotted as a number out of 100 simulations.

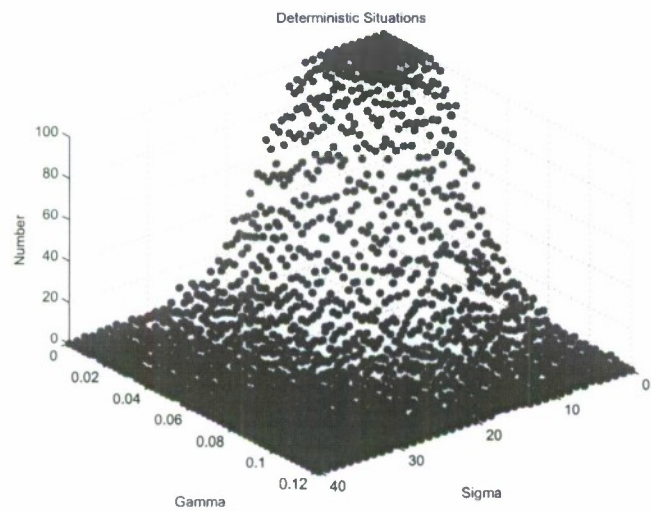


Figure 7: The (σ, γ) essentially deterministic surface along $\sigma \in [0, 40]$, $\gamma \in [0, 0.12]$ plotted as a number out of 100 simulations.

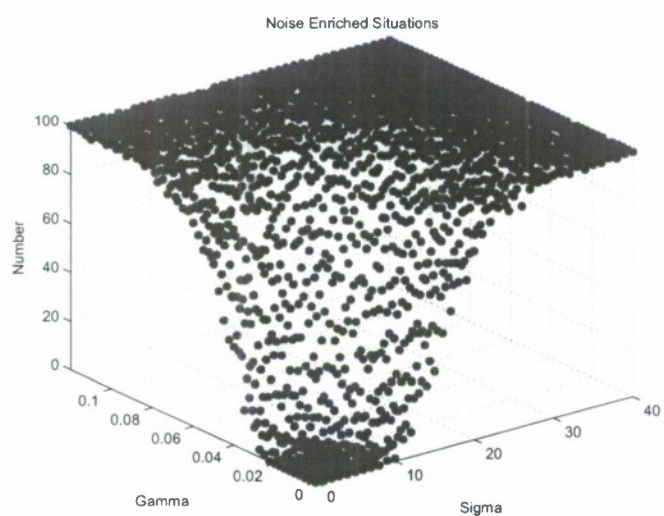


Figure 8: The (σ, γ) noise enriched surface along $\sigma \in [0, 40]$, $\gamma \in [0, 0.12]$ plotted as a number out of 100 simulations.

4.2.7 Stochastic Model with Smooth Coefficients

The coupled SDE model with smooth coefficients were also used to simulate the case denoted above and produced visually identical results. In the deterministic case, the values of b that control clustering behavior are identical to those found in the deterministic case of the basic SDE system; that is, one cluster formed when $b \in (0, 0.00155)$; two clusters formed when $b \in [0.00155, 0.01390]$; and three clusters formed when $b \in [0.01390, \infty)$. The sample distributions of regimes also appear to be very similar to those established in [7]. Instead of using agent 10 to represent all agents j with $C_j(0) = (10, 10)$, agent 1 was used with no impact of the behavior of the model.

To verify that the model exhibited random behavior when $\sigma \neq 0$ and $\gamma \neq 0$, a simulation of the one-cluster scenario was run using the parameters $\sigma = 5$ and $\gamma = 1$. The general behavior exhibited by the deterministic case is also evident in this stochastic case. Note that the trend of increasing connectivities in a one-cluster deterministic case, pictured in Figure 4.2.7, is also reflected in the one-cluster stochastic case pictured in Figure 4.2.7. Also, the tendency for characteristic values in the one-cluster deterministic case to approach a certain value between all the characteristic values, shown in Figure 4.2.7, is also present in the one-cluster stochastic case, as illustrated by Figure 4.2.7.

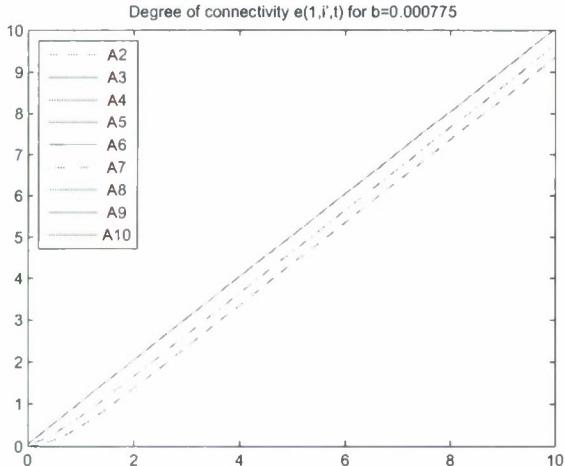


Figure 9: Degree of connectivity $e(1, i', t)$, $i' \neq 1$ of agent 1 with other agents for $b = 0.000775$, $\sigma = 0$, and $\gamma = 0$ using the smooth coefficient model (one cluster scenario, deterministic case).

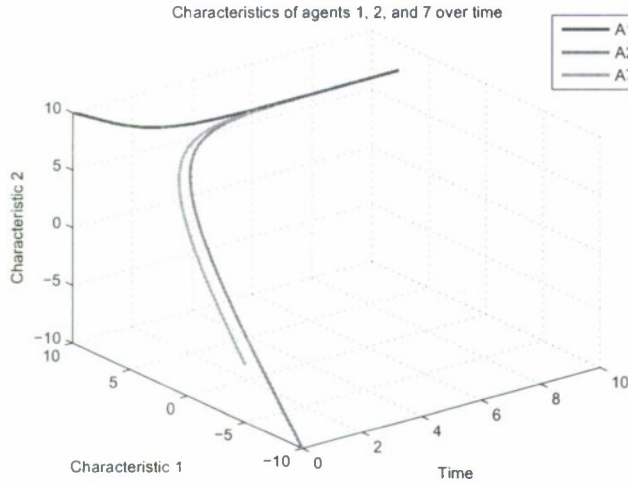


Figure 10: Characteristic values of agents 1, 2, and 7 over $t \in [0, 10]$ for $b = 0.000775$, $\sigma = 0$, and $\gamma = 0$ (one cluster scenario, deterministic case).

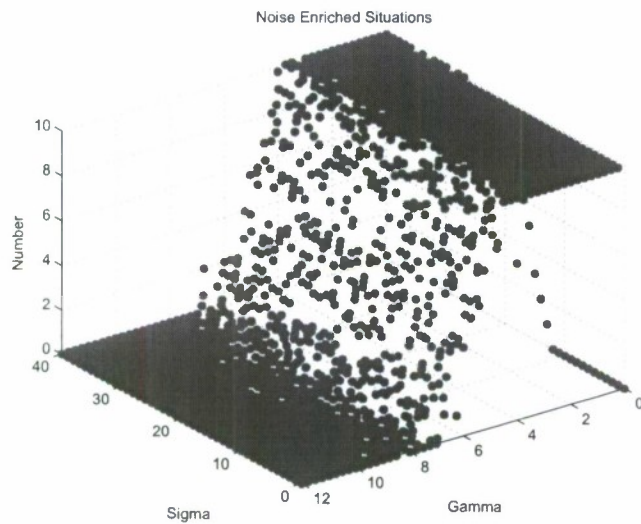


Figure 11: The (σ, γ) noise enriched surface along $\sigma \in [0, 40]$, $\gamma \in [0, 12]$ plotted as a number out of 10 simulations using the smooth coefficient model.

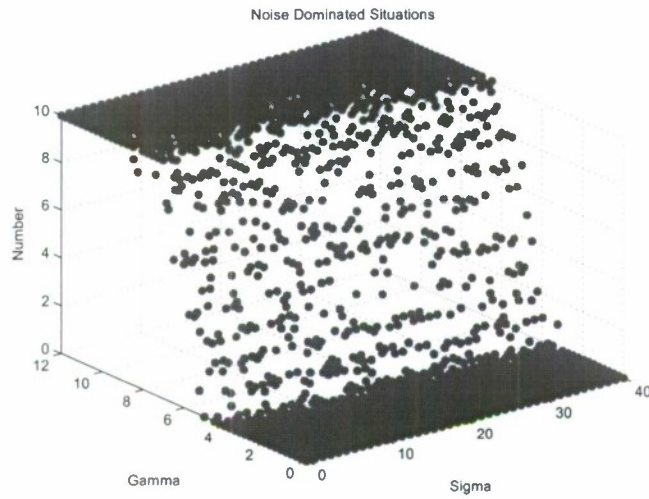


Figure 12: The (σ, γ) noise dominated surface along $\sigma \in [0, 40]$, $\gamma \in [0, 12]$ plotted as a number out of 10 simulations using the smooth coefficient model.

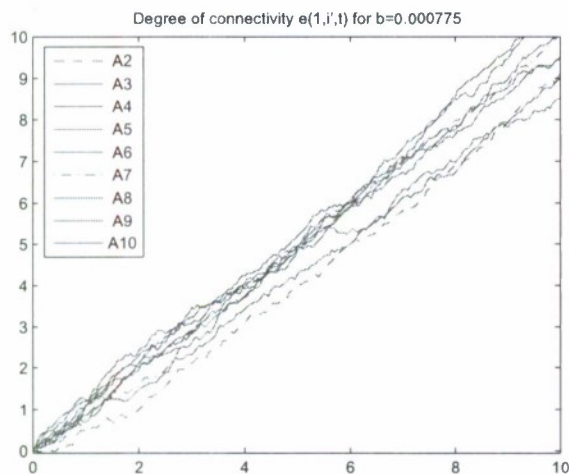


Figure 13: Degree of connectivity $e(1, i', t)$, $i' \neq 1$ of agent 1 with other agents for one trial using the parameters $b = 0.000775$, $\sigma = 5$, and $\gamma = 1$ using the smooth coefficient model (one cluster scenario, stochastic case).

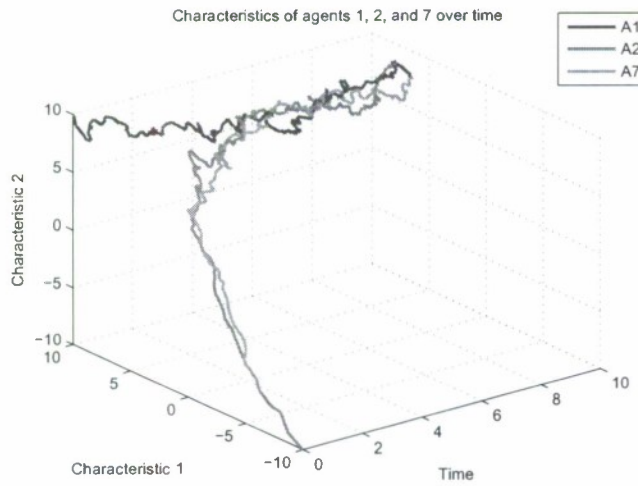


Figure 14: Characteristic values of agents 1, 2, and 7 over $t \in [0, 10]$ for one trial using the parameters $b = 0.000775$, $\sigma = 5$, and $\gamma = 1$ (one cluster scenario, stochastic case).

4.2.8 Fokker-Planck Equivalent Formulation

With the establishment of the smooth SDE model and its faithfulness to the SDE model first proposed by [7], the development of an equivalent FP model may proceed. Let $\{X(t)\}$ be a stochastic process, with $t \in [t_0, \infty)$, and $X(t)$ a random variable continuous in time and state, $X(t) \in (-\infty, \infty)$. Let $X(t)$ satisfy the *Ito SDE*

$$dX(t) = \alpha(X(t), t)dt + \beta(X(t), t)dW(t), \quad (4.13)$$

where $dW(t)$ represents an infinitesimal Wiener increment, and $W(t)$ is the standard Wiener process. The mean and variance of $X(t)$ is then $\alpha(X(t), t)$ and $\beta^2(X(t), t)$, respectively. Conditions (4.14) - (4.16)

$$\lim_{\Delta t \rightarrow 0} \frac{1}{\Delta t} \int_{-\infty}^{\infty} |y - x|^\delta p(y, t + \Delta t; x, t) dy = 0, \quad \delta > 2 \quad (4.14)$$

$$\lim_{\Delta t \rightarrow 0} \frac{1}{\Delta t} \int_{-\infty}^{\infty} (y - x)p(y, t + \Delta t; x, t) dy = \alpha(x, t), \quad (4.15)$$

$$\lim_{\Delta t \rightarrow 0} \frac{1}{\Delta t} \int_{-\infty}^{\infty} (y - x)^2 p(y, t + \Delta t; x, t) dy = \beta^2(x, t), \quad (4.16)$$

establish the smoothness of coefficients $\alpha(X(t), t)$ and $\beta(X(t), t)$. Should these conditions be satisfied, it can be shown via the application of the Chapman-Kolmogorov equation and Taylor expansion of a test function, that $X(t)$ is a diffusion process. Equivalently, this means that $X(t)$ satisfies the Kolmogorov equations with drift coefficient α and diffusion coefficient β^2 . The corresponding forward Kolmogorov (or Fokker-Planck) equation is then

$$\frac{\partial p}{\partial t} = -\frac{\partial(\alpha(x, t)p)}{\partial x} + \frac{1}{2} \frac{\partial^2(\beta^2(x, t)p)}{\partial x^2}. \quad (4.17)$$

In equation (4.17), p is the pdf of the stochastic process $X(t)$, and the transition from state x at time t to state y at time s is then $p(y, s; x, t)$.

Generalizing (4.17) to M dimensions as in [22], we find the forward Kolmogorov/Fokker-Planck is given by

$$\frac{\partial p}{\partial t} = -\sum_{i=1}^M \frac{\partial}{\partial x_i} [S_i p] + \frac{1}{2} \sum_{i,j=1}^M \frac{\partial^2}{\partial x_i \partial x_j} [S_{ij} p], \quad (4.18)$$

where $\mathbf{X} = (X_1, \dots, X_M)$ is a stochastic process such that

$$S_i = \lim_{\Delta t \rightarrow 0} \frac{1}{\Delta t} E[\Delta X_i(t) | X_i(t) = x_i],$$

and

$$S_{ij} = \lim_{\Delta t \rightarrow 0} \frac{1}{\Delta t} E[\Delta X_i(t) \Delta X_j(t) | X_i(t) = x_i, X_j(t) = x_j].$$

If we let $C_i^k(t)$ represent the k th element of $\mathbf{C}_i(t)$, and apply (4.18), the forward Kolmogorov formulation corresponding to model (4.9) - (4.10) is then

$$\begin{aligned} \frac{\partial p}{\partial t} = & - \sum_{i=1}^N \frac{\partial}{\partial C_i^1} \left[\left(\frac{\beta_i}{\sum_{\phi_i} e(i, i', t)} \sum_{\phi_i} e(i, i', t) [C_{i'}^1(t) - C_i^1(t)] \right) p \right] \\ & - \sum_{i=1}^N \frac{\partial}{\partial C_i^2} \left[\left(\frac{\beta_i}{\sum_{\phi_i} e(i, i', t)} \sum_{\phi_i} e(i, i', t) [C_{i'}^2(t) - C_i^2(t)] \right) p \right] \\ & - \dots - \sum_{i=1}^N \frac{\partial}{\partial C_i^m} \left[\left(\frac{\beta_i}{\sum_{\phi_i} e(i, i', t)} \sum_{\phi_i} e(i, i', t) [C_{i'}^m(t) - C_i^m(t)] \right) p \right] \\ & + \sum_{i=1}^N \sum_{i'=1}^N \frac{\partial}{\partial e_{i,i'}} [f(\|\mathbf{C}_{i'}(t) - \mathbf{C}_i(t)\|^2)p] \\ & + \frac{1}{2} \sum_{i=1}^N \frac{\partial^2(\sigma^2 p)}{\partial(C_i^1)^2} + \sum_{i=1}^N \frac{\partial^2(\sigma^2 p)}{\partial(C_i^2)^2} + \dots + \sum_{i=1}^N \frac{\partial^2(\sigma^2 p)}{\partial(C_i^m)^2} + \sum_{i=1}^N \sum_{i'=1}^N \frac{\partial^2(\gamma^2 p)}{\partial e_{i,i'}^2}. \end{aligned}$$

Here p is the joint transition probability density function of $p(\mathbf{C}_i(t), e(i, i', t), t)$. Summing the drift of $C_i^k(t)$ and the variances of the Wiener processes for each characteristic results in

$$\begin{aligned} \frac{\partial p}{\partial t} = & - \sum_{i=1}^N \sum_{k=1}^m \frac{\partial}{\partial C_i^k} \left[\left(\frac{\beta_i}{\sum_{\phi_i} e(i, i', t)} \sum_{\phi_i} e(i, i', t) [C_{i'}^k(t) - C_i^k(t)] \right) p \right] \\ & + \sum_{i=1}^N \sum_{i'=1}^N \frac{\partial}{\partial e_{i,i'}} [f(\|\mathbf{C}_{i'}(t) - \mathbf{C}_i(t)\|^2)p] \\ & + \frac{1}{2} \sum_{i=1}^N \sum_{k=1}^m \frac{\partial^2(\sigma^2 p)}{\partial(C_i^k)^2} + \sum_{i=1}^N \sum_{i'=1}^N \frac{\partial^2(\gamma^2 p)}{\partial e_{i,i'}^2}. \end{aligned} \tag{4.19}$$

4.2.9 Finite Difference Scheme for Fokker-Planck Model

The finite difference approximation formulated by [14] preserves the properties of the FP model. This numerical scheme yields a non-negative solution for all values of \bar{x} , conserves the area of the p.d.f. p , and is known to be relatively stable. Additionally, this method allows mesh points to be more widely spaced than in some competing methods. Define the

following functions

$$\begin{aligned} G(\bar{x}, t) &= \sum_{i=1}^N \sum_{k=1}^m \frac{-\beta}{\sum_{\phi_i} e(i, i', t)} \sum_{\phi_i} e(i, i', t) [\mathbf{C}_{i'}^k(t) - \mathbf{C}_i^k(t)] \\ &\quad + \sum_{i=1}^N \sum_{i'=1}^N 2 [\exp(-b||\mathbf{C}_i(t) - \mathbf{C}_{i'}(t)||^2) - 1] \end{aligned} \quad (4.20)$$

$$F(\bar{x}, t) = Gp + \frac{\sigma^2}{2} \sum_{i=1}^N \sum_{k=1}^m \frac{\partial p}{\partial C_i^k(t)} + \frac{\gamma^2}{2} \sum_{i=1}^N \sum_{i'=1}^N \frac{\partial p}{\partial e(i, i', t)} \quad (4.21)$$

For any $x \in \bar{x}$, let $\Delta x = (x_{max} - x_{min})/R$, where x_{max} and x_{min} are the upper and lower boundaries of the domain of $x \in \bar{x}$ and R is the number of intervals into which the domain of x shall be divided. Let $\Delta t = T/S$, where S is the number of time steps. The mesh points shall be given by $x_r = x_{min} + r\Delta x$, $r = 0, 1, 2, \dots, R$ and $t_s = s\Delta t$, $s = 0, 1, 2, \dots, S$. The midpoint between two mesh points in x can be interpolated linearly by $x_{r+\frac{1}{2}} = \frac{x_r + x_{r+1}}{2}$. The approximation (4.21) may be utilized to obtain

$$\frac{p_r^{s+1} - p_r^s}{\Delta t} = \frac{F_{r+\frac{1}{2}}^{s+1} - F_{r-\frac{1}{2}}^{s+1}}{\Delta x} \quad (4.22)$$

where $p_r^{s+1} - p_r^s$ denotes the change of the p.d.f. p w.r.t. the change in $x \in \bar{x}$ from one mesh point to the proceeding mesh point. Letting $\lambda = \sigma$ if $x \in \bar{C}$ and $\lambda = \gamma$ if $x \in \bar{e}$, $F_{r+\frac{1}{2}}^{s+1}$ may be defined as

$$\begin{aligned} F_{r+\frac{1}{2}}^{s+1} &= G_{r+\frac{1}{2}}^{s+1} p_{r+\frac{1}{2}}^{s+1} + \frac{\lambda^2}{2} \frac{p_{r+1}^{s+1} - p_r^{s+1}}{\Delta x} \\ &= G_{r+\frac{1}{2}}^{s+1} [\delta_r^{s+1} p_{r+1}^{s+1} + (1 - \delta_r^{s+1}) p_r^{s+1}] + \frac{\lambda^2}{2} \frac{p_{r+1}^{s+1} - p_r^{s+1}}{\Delta x} \\ &= \left[\delta_r^{s+1} G_{r+\frac{1}{2}}^{s+1} + \frac{\lambda^2}{2\Delta x} \right] p_{r+1}^{s+1} + \left[(1 - \delta_r^{s+1}) G_{r+\frac{1}{2}}^{s+1} - \frac{\lambda^2}{2\Delta x} \right] p_r^{s+1} \end{aligned} \quad (4.23)$$

$$\text{where } \delta_r^{s+1} = \frac{1}{\tau_r^{s+1}} - \frac{1}{\exp(\tau_r^{s+1}) - 1}, \quad \tau_r^{s+1} = \frac{G_{r+\frac{1}{2}}^{s+1} \Delta x}{\lambda^2}$$

To preserve the zero-flux boundary conditions of $F(\bar{x}|x_{min} \in \bar{x}, t_{s+1}) = 0$ and $F(\bar{x}|x_{max} \in \bar{x}, t_{s+1}) = 0$, let $F_{-\frac{1}{2}}^{s+1} = 0$ and $F_{r+\frac{1}{2}}^{s+1} = 0$. Equation (4.22) can be solved using the system

$$-\phi_{1,r}^{s+1} p_{r+1}^{s+1} + \phi_{0,r}^{s+1} p_r^{s+1} - \phi_{-1,r}^{s+1} p_{r-1}^{s+1} = p_r^s \quad (4.24)$$

where

$$\begin{aligned}\phi_{1,r}^{s+1} &= \frac{\Delta t}{\Delta x} \left[\frac{\lambda^2}{4\Delta x} - \delta_r^{s+1} G_{r+\frac{1}{2}}^{s+1} \right] \\ \phi_{0,r}^{s+1} &= 1 + \frac{\Delta t}{\Delta x} \left[(1 - \delta_r^{s+1}) G_{r+\frac{1}{2}}^{s+1} - \delta_{r+1}^{s+1} G_{r-\frac{1}{2}}^{s+1} \right] + \frac{\lambda^2 \Delta t}{2\Delta x^2} \\ \phi_{-1,r}^{s+1} &= \frac{\Delta t}{\Delta x} \left[(1 - \delta_r^{s+1}) G_{r+\frac{1}{2}}^{s+1} + \frac{\lambda^2}{4\Delta x} \right]\end{aligned}$$

4.2.10 Conclusions to Date

The results found in [7] were successfully duplicated using a modified version of the model. The coupled SDE model proposed in [7] can be converted to an SDE model with smooth coefficients. Equation (4.6) originally possessed smooth coefficients, and to change (4.5) to be composed of only smooth coefficients involved scaling the difference in two agents' characteristic values by the connectivity between those two agents if the connectivity is positive. Other methods of smoothing the coefficients were considered but did not fulfill the requirement of homophily between agents. Changing the system (4.5)-(4.6) to (4.9)-(4.10) we found no discernable change in model behavior in both deterministic and stochastic cases and no change in the effect of parameters β and b or variables σ and γ on the system.

With smooth coefficients, the SDE fulfills the definition of a diffusion process, thus allowing an equivalent multidimensional Fokker-Planck (FP) model to be formulated from the coupled SDE system (4.9) - (4.10). Usage of the FP model is nearly ubiquitous in many scientific fields, and current research is being performed to further develop and understand the FP equation [3]. The FP formulation possesses drift coefficients as described in (4.20) and diffusion coefficients equal to σ in Nm dimensions of the process and γ in an additional $N(N - 1)$ dimensions. It is possible to approximate the FP model by a Finite Difference Scheme; however, the ability and computational efficiency of such a method, while still under investigation, are less than promising. In response to the conclusions of these investigations, it was decided that additional model complexity will be incorporated and delays will be added directly to the SDE model.

4.2.11 Social Network Model with Delay

In a first step, the version of the stochastic social network model discussed above and in [8] can be generalized with a single discrete delay is

$$\begin{aligned}\dot{C}_i(t) &= \frac{\beta_i}{\sum_{i' \in A_i(t-\tau)} e_i(i', t - \tau)} \sum_{i' \in A_i(t-\tau)} e_i(i', t - \tau) [C_{i'}(t - \tau) - C_i(t - \tau)] \quad (4.25) \\ \dot{e}(i, i', t) &= f(\|C_i(t) - C_{i'}(t)\|^2)\end{aligned}$$

where $f(\xi) = 2e^{-b\xi} - 1$ and $\phi = e(i, i', t - \tau)$. This system is for $i = 1, \dots, m$ where m is the number of agents considered, $C_i(t)$ denotes the value(s) of the k characteristics of the agents, and $e(i, i', t)$ the strength of the connections between the agents.

We are currently using delay equation numerical approximation techniques [1, 6] developed under previous AFOSR support to explore features of these models with delays. We note the dimension of the approximating ODE system is then $n = km + m^2 = m(k + m)$. Results will be reported in [9].

References

- [1] H.T. Banks, Identification of nonlinear delay systems using spline methods, *Proc. Intl. Conf. on Nonlinear Phenomena in Mathematical Sciences* (V. Lakshmikantham, Ed.), Academic Press, (1982), 47–55.
- [2] H. T. Banks, D. Bortz, G. A. Pinter and L. K. Potter, Modeling and imaging techniques with potential for application in bioterrorism, Chapter 6 in *Bioterrorism: Mathematical Modeling Applications in Homeland Security*, H.T. Banks and C. Castillo-Chavez, eds., Frontiers in Applied Mathematics, SIAM, Philadelphia, 2003, pp. 129–154.
- [3] H.T. Banks, J.L. Davis and Shuhua Hu, Comparison of Fokker-Planck model and growth rate distribution model in modeling growth uncertainty, in preparation.
- [4] H. T. Banks, S. Dediu and S. L. Ernstberger, Sensitivity functions and their uses in inverse problems, CRSC-TR07-12, July, 2007; *J. Inverse and Ill-posed Problems*, **15** (2007), 683–708.
- [5] H.T. Banks, S. Dediu, S.L. Ernstberger and Franz Kappel, A new approach to optimal design problems, CRSC-TR08-12, September, 2008; *Inverse Problems*, submitted.
- [6] H. T. Banks and F. Kappel, Spline approximations for functional differential equations, *Journal of Differential Equations*, **34** (1979), 496–522.
- [7] H.T. Banks, A.F. Karr, H.K. Nguyen and J.R. Samuels, Jr., Sensitivity to noise variance in a social network dynamics model, CRSC-TR05-41, November, 2005; *Quarterly Applied Math*, **66** (2008), 233–247.
- [8] H. T. Banks, K. L. Rehm, and K. L. Sutton, *Conversion of Dynamic Social Network Stochastic Differential Equation Model to Fokker-Planck Model*, REG-NSF summary report, North Carolina State University, August, 2008.
- [9] H. T. Banks, K. L. Rehm, K. Sutton, Dynamic social network models with stochasticity and delays, in preparation.

- [10] P. Bai, H. T. Banks, S. Dediu, A. Y. Govan, M. Last, A. Loyd, H. K. Nguyen, M. S. Olufsen, G. Rempala and B. D. Slenning, Stochastic and deterministic models for agricultural production networks, *Math. Biosci. and Engineering*, **4** (2007), 373–402.
- [11] J. J. Batzel, F. Kappel, D. Schneditz and H.T. Tran, *Cardiovascular and Respiratory Systems: Modeling, Analysis and Control*, SIAM Frontiers in Applied Math, SIAM, Philadelphia, 2006.
- [12] M. P. F. Berger and W. K. Wong (Editors), *Applied Optimal Designs*, John Wiley & Sons, Chichester, UK, 2005.
- [13] G. Casella and R. L Berger, *Statistical Inference*, Duxbury, CA, 2002.
- [14] J.S. Chang and G. Cooper, A practical difference scheme for Fokker-Planck equations, *Journal of Computational Physics*, **6** (1970), 1–16.
- [15] M. Davidian and D.M. Giltinan, *Nonlinear Models for Repeated Measurement Data*, Chapman and Hall, London, 1995.
- [16] S. N. Ethier and T. G. Kurtz, *Markov Processes: Characterization and Convergence*, J. Wiley & Sons, New York, 1986.
- [17] V. V. Fedorov, *Theory of Optimal Experiments*, Academic Press, New York and London, 1972.
- [18] V. V. Fedorov and P. Hackel, *Model-Oriented Design of Experiments*, Springer-Verlag, New York, NY, 1997.
- [19] A. R. Gallant, *Nonlinear Statistical Models*, John Wiley & Sons, Inc., NY, 1987.
- [20] M. Handcock, Progress in statistical modeling of drug user and sexual networks, University of Washington Report, 2000.
- [21] B. Oksendal, *Stochastic Differential Equations*, 5th edition, Springer, Berlin, 2000.
- [22] R.F. Pawula, Generalizations and extensions of the Fokker-Planck-Kolmogorov equations, *IEEE Transactions on Information Theory*, **IT-13** (1967), 33–41.
- [23] Yu. V. Prohorov, Convergence of random processes and limit theorems in probability theory, *Theor. Prob. Appl.*, **1** (1956), 157–214.
- [24] F. Pukelsheim, *Optimal Design of Experiments*, John Wiley & Sons, New York, NY, 1993.
- [25] G. A. F. Seber and C. J. Wild, *Nonlinear Regression*, John Wiley & Sons, Inc., New York, 1989.
- [26] K. Thomaseseth and C. Cobelli, Generalized sensitivity functions in physiological system identification, *Ann. Biomed. Eng.*, **27** (1999), 607–616.